# Structural Markers Observed with Endoscopic Three-dimensional Optical Coherence Tomography Correlating with Barrett's Esophagus Radiofrequency Ablation Treatment Response

**Tsung-Han Tsai, MS**,
Department of Electrical Engineering & Computer Science, Research Laboratory of Electronics, Massachusetts Institute of Technology, Cambridge, MA, USA

**Chao Zhou, PhD**,
Department of Electrical Engineering & Computer Science, Research Laboratory of Electronics, Massachusetts Institute of Technology, Cambridge, MA, USA

**Yuankai K. Tao, PhD**,
Department of Electrical Engineering & Computer Science, Research Laboratory of Electronics, Massachusetts Institute of Technology, Cambridge, MA, USA

**Hsiang-Chieh Lee, MS**,
Department of Electrical Engineering & Computer Science, Research Laboratory of Electronics, Massachusetts Institute of Technology, Cambridge, MA, USA

**Osman O. Ahsen, BS**,
Department of Electrical Engineering & Computer Science, Research Laboratory of Electronics, Massachusetts Institute of Technology, Cambridge, MA, USA

**Marisa Figueiredo, PA**,
VA Healthcare System Boston, Boston, MA, USA; Harvard Medical School, Boston, MA, USA

**Tejas Kirtane, MD**,
VA Healthcare System Boston, Boston, MA, USA; Harvard Medical School, Boston, MA, USA

**Desmond C. Adler, PhD**,
LightLab Imaging Inc. - St Jude Medical, Inc., Westford, MA, USA

**Joseph M. Schmitt, PhD**,
LightLab Imaging Inc. - St Jude Medical, Inc., Westford, MA, USA

**Qin Huang, MD**,
VA Healthcare System Boston, Boston, MA, USA; Harvard Medical School, Boston, MA, USA

**James G. Fujimoto, PhD**, and
Department of Electrical Engineering & Computer Science, Research Laboratory of Electronics, Massachusetts Institute of Technology, Cambridge, MA, USA

**Hiroshi Mashimo, MD, PhD**

Correspondence to: Hiroshi Mashimo, MD, PhD, Gastroenterology Section, VA Boston Healthcare System, Harvard School of Medicine, Boston, MA, 02130. hmashimo@hms.harvard.edu, Telephone: +1-857-203-5640, Fax: +1-857-203-5666.

VA Healthcare System Boston, Boston, MA, USA; Harvard Medical School, Boston, MA, USA

## Abstract

**Background—**Radiofrequency ablation (RFA) is effective for treating Barrett's esophagus (BE) but often involves multiple endoscopy sessions over several months to achieve complete response.

**Objective—**Identify structural markers using three-dimensional optical coherence tomography (3D-OCT) that correlate with treatment response.

**Design—**Cross-sectional.

**Setting—**Single teaching hospital.

**Patients—**Thirty-two male and one female Caucasians with short-segment BE (<3cm) undergoing RFA treatment.

**Interventions—**Patients were treated with focal RFA and 3D-OCT was performed at the gastroesophageal junction before and immediately after the RFA treatment. Patients were re-examined with standard endoscopy 6-8 weeks later and biopsied to rule out BE if not visibly evident.

**Main outcome measurement—**The thickness of BE epithelium before RFA and the presence of residual-gland-like structures immediately after RFA were determined using 3D-OCT. The presence of BE at follow-up was assessed endoscopically.

**Results—**BE mucosa was significantly thinner in patients who achieved complete eradication of intestinal metaplasia (CE-IM) than in patients who did not achieve CE-IM at follow-up [$257\pm60\mu$m vs. $403\pm86\mu$m, p<0.0001]. A threshold thickness of $333\mu$m derived from receiver-operator characteristics corresponds to a 92.3% sensitivity, 85% specificity and 87.9% accuracy in predicting the presence of BE at follow-up. The presence of OCT-visible glands immediately after RFA also correlated with the presence residual BE at follow-up (83.3% Sensitivity, 95% specificity, and 90.6% accuracy).

**Limitations—**Single center, cross sectional study and only patients with short-segment BE were examined.

**Conclusions—**3D-OCT assessment of BE thickness and residual glands during RFA sessions correlated with treatment response. 3D-OCT may predict response to RFA or make real-time RFA retreatment decisions in the future.

### Keywords

Optical Coherence Tomography; Optical Biopsy; Barrett's Esophagus; Radiofrequency Ablation; Epithelial depth

## Introduction

Radiofrequency ablation (RFA) is an emerging endoscopic therapy for treating Barrett's esophagus (BE).[1-5] Utilizing electrode arrays, RFA catheters deliver radiofrequency energy to the surface of esophageal tissues to ablate BE with a low stricture rate.[6, 7] Recent studies have shown that at one year follow-up from the initial RFA treatment, complete eradication of dysplasia (CE-D) was achieved in 90.5% of patients with low grade dysplasia (LGD) and in 81% of patients with high grade dysplasia (HGD).[4] At two year follow-up, CE-D was achieved in 98% and 93% of patients with LGD and HGD, respectively.[8] Complete eradication of intestinal metaplasia (CE-IM) was achieved in 93% of the patients with dysplasia after two years[8] and in 92% of patients with non-dysplastic BE (NDBE) at 5-year

follow-up.[9] However, recurrence of intestinal metaplasia (IM) was observed in 13%[8] and even 25.9%[10] of patients at 1 year after CE-IM was achieved. It is unclear what risk factors are associated with the recurrence of IM.

Repeated RFA treatments are generally required to achieve complete eradication of aberrant tissues.[11-13] On average, CE-IM was achieved after 3.4 RFA sessions for patients with NDBE[9] and over 3.5 sessions for patients with dysplasia.[4, 8] Considering the follow up time between RFA procedures (usually 6-8 weeks), the entire treatment process can easily span half a year or longer. In addition, the cost to achieve complete eradication mounts with each esophagogastroduodenoscopy (EGD) and RFA procedure, and has tempered the enthusiasm to treat all NDBE using RFA.[14, 15] Therefore, improving the effectiveness of each RFA procedure would reduce the number of treatment sessions, improve cost effectiveness, reduce patient anxiety and make this therapy available to a wider patient population.

Optical coherence tomography (OCT) is a volumetric imaging technique that generates cross-sectional and 3D images of tissue microstructures with micron scale resolution.[16] Endoscopic OCT techniques have been developed to image the human gastrointestinal (GI) tract with over 1 mm imaging depth.[17-26] Two-dimensional OCT has been used to evaluate specialized intestinal metaplasia, dysplasia, and adenocarcinoma in the esophagus and has achieved a high sensitivity and specificity to differentiate different pathologies.[22, 27] Recently, endoscopic 3D-OCT has become possible due to dramatic increases in imaging speed.[23-26] 3D-OCT provides a powerful combination of high resolution, large field of view, and rapid data acquisition. 3D-OCT has been used to image patients with upper and lower GI diseases.[23, 26] Recent studies demonstrated that 3D-OCT can identify buried glands before and after CE-IM from RFA treatment.[23, 28] The objective of this investigation was to identify possible structural markers that predict RFA treatment response using endoscopic 3D-OCT.

## Methods

### Patient Enrollment and Study Protocol

This study was conducted at the Veterans Affairs Boston Healthcare System (VABHS), Jamaica Plain Campus over the past 2 years. The study protocol was approved by the VABHS, Harvard Medical School and Massachusetts Institute of Technology. Patients were diagnosed with standard white light endoscopy and the length of visible BE was recorded based on the Prague C&M criteria.[29] Thirty-three patients with short-segment BE (<3 cm), including one female, were recruited for this study. The study also included patients who initially presented with long segment BE that were reduced to less than 3 cm segment by prior circumferential RFA treatment using the BARRX Halo360™ catheter. Informed consent was obtained from each patient. Only patients with short-segment BE were imaged in order to ensure consistent OCT imaging catheter placement at the gastroesophageal junction (GEJ) and ascertaining presence of BE, thickness, and residual glands relative to the GEJ within the OCT pullback image. This study focused on patients receiving ablation with the Halo90™ catheter. For each RFA treatment, the patient received two sets of ablations using the BARRX Halo90™ catheter (300 Watts at 12 J/cm$^2$ for each set of ablations), with rigorous scraping to remove desquamated epithelium between the two ablations, per standard protocol set by the manufacture. Patients with circumferential short-segment BE were also treated using Halo90™ catheter in order to maintain consistent procedure and ablation energy level. After the RFA, patients received a proton pump inhibitor (PPI), i.e., 40 mg of esomeprazole or omeprazole bid. At 6-8 weeks follow-up, the presence of residual BE was evaluated using white light endoscopy and narrow band imaging (NBI), as well as random 4-quandrant pinch biopsies. If no visible BE was observed endoscopically and no IM was found from biopsies at the GEJ the patient was

classified as CE-IM. There were 13 patient in the CE-IM Group and 20 patients in the Non-CE-IM Group in this study.

## Endoscopic 3D-OCT Imaging

A prototype endoscopic 3D-OCT system,[25, 30] developed by LightLab Imaging - St Jude Medical (Westford, Massachusetts, USA), was used for this study. The system had a lateral resolution of 15 µm, an axial resolution of 5 µm and imaging depth of ~2 mm in tissue. 3D-OCT imaging was performed with the OCT catheter introduced through the biopsy channel of the endoscope (GIF Q180; Olympus, Tokyo, Japan), enabling simultaneous video endoscopy. Volumetric OCT data was acquired at 60,000 axial lines per second and 60 frames per second. The imaging catheter scanned a helical pull back pattern with an 8 mm circumference and 20 mm pullback length within 20 seconds. The endoscope was at the neutral position with the imaging catheter placed at 6 o'clock in the endoscopic field. The imaging catheter was in contact with the esophagus and the pull back imaging spanned the GEJ. The esophagus was deflated and naturally wrapped around the OCT catheter during imaging acquisition to maintain a consistent catheter contact for all patients. Multiple 3D-OCT datasets were acquired at the GEJ before and immediately after the RFA treatment.

## Image Analysis

Each 3D-OCT data set was reviewed and analyzed using 3D rendering software (Amira, Visage Imaging, Inc.). The BE epithelium thickness was measured from cross-sectional OCT images obtained prior to the RFA treatment. As indicated in Figure 1, the BE thickness was measured as the vertical distance from the top of the lamina propria (LP) / muscularis mucosa (MM) layer to the surface of the BE epithelium at the center position where the OCT catheter had the best contact with the esophagus. Multiple BE thickness measurements were obtained from each 3D data set every 1 mm along the entire BE length. The average and maximum BE thickness were recorded for each patient for statistical comparison between the CE-IM and Non-CE-IM groups.

In addition, two types of residual glandular structures were observed by reviewing 3D-OCT images obtained immediately after the second RFA. The first type of glandular structure was unburned BE epithelium that was likely missed by RFA and showed similar epithelial structure as that of regular BE. The second type of glandular structure consisted of hyposcattering glandular structures above the LP/MM layer at the RFA treatment site, representing residual glands. The presence or absence of these residual glands was recorded for each patient.

## Statistical Analysis

The primary study outcome was to determine the accuracy of using BE thickness measured with OCT prior to RFA to predict the treatment response (presence or absence of endoscopically visible residual BE at follow-up). A Student's t-test was used to compare the average and maximum BE thickness from the CE-IM and Non-CE-IM groups. To evaluate whether BE thickness can be used to predict the RFA treatment response, receiver operator characteristic (ROC) curves were plotted by using a discrimination threshold ranging from 100 µm to 800 µm for average and maximum BE thickness, respectively. A decision threshold was determined from the ROC curves to achieve maximum overall accuracy. Sensitivity, specificity, positive predicting value (PPV), negative predicting value (NPV) and accuracy of the prediction was then calculated.

The secondary study outcome was to evaluate the correlation between the presence or absence of residual glands on OCT imaging immediately after RFA versus RFA treatment response assessed endoscopically on follow up. In addition, we also evaluated the

correlation between the BE thickness prior to RFA versus the presence or absence of residual glands immediately after RFA. The sensitivity, specificity, PPV, NPV and the accuracy were calculated.

All statistical analyses were performed using MATALB software (Mathworks Inc.). All tests were two-sided and a p value of < 0.05 was considered statistically significant.

## Results

Table 1 lists demographic information of the patients enrolled in this study. The average age for the CE-IM and Non-CE-IM groups were comparable (p=0.86). The CE-IM group consisted of 13 patients (4 patients had BE without dysplasia, 2 BE with low-grade dysplasia and 7 BE with high-grade dysplasia at presentation). The Non-CE-IM group consisted of 20 patients (10 patients had BE without dysplasia, 4 BE with low-grade dysplasia and 6 BE with high-grade dysplasia at presentation). Patients in the Non-CE-IM group are presumed to eventually have a treatment response with additional RFA treatments and convert to the CE-IM group and investigation of this group is ongoing. The number of prior RFA treatments and the length of BE was not statistically different between the two groups. There were no adverse events after RFA treatment.

Figure 1A shows an example endoscopic image of the GEJ before applying focal RFA treatment. 3D-OCT imaging was performed at the GEJ over the area of BE (pink colored). Figure 1B shows a representative cross-sectional OCT image obtained at the GEJ prior to the RFA treatment, together with histology obtained from the same site (Figure 1C). The thickness of the BE epithelium was measured from the OCT image as distance between the BE surface to the top of the LP / MM layer.

Figure 2A shows an example endoscopic image of the GEJ immediately after focal RFA treatment with scraping to remove desquamated epithelium between first and second RFA application. The RFA treated area was covered with blood and burned tissue, making it difficult to identify residual BE patches on white light endoscopy or NBI. Figure 2B shows a representative cross-sectional OCT image obtained immediately after RFA. Similar epithelium structure was observed compared to Figure 1B, indicating the presence of residual BE that was missed by the RFA treatment. A video of cross-sectional OCT images scanning through the unburned BE area is provided in the Supplemental Materials (Video S1). Another type of residual glandular structure usually can be observed after insufficient power delivery on the tissue, leading to hyposcattering features above the LP/MM layer at the RFA treated site in OCT images. Figure 2C shows residual glands (red arrows) above the MM layer, suggesting these glands were not effectively removed by the RFA treatment. A biopsy was taken from the same site immediately after the OCT imaging and confirmed the presence of residual BE glands immediately after the RFA treatment (Figure 2D). A video of cross-sectional OCT images scanning through these residual BE glands is provided in the Supplemental Materials (Video S2). Figure 2E shows a representative OCT image demonstrating effective RFA treatment, where the MM layer was on top of the tissue surface with no epithelial structures above it. A video of cross-sectional OCT images scanning through the effectively treated area is provided in the Supplemental Materials (Video S3).

The BE thickness measured with OCT prior to RFA was found to be a predictor of the RFA treatment response. Both the average and maximum BE thickness prior to RFA were significantly thinner for the CE-IM group compared to the Non-CE-IM group [Average BE thickness, $257\pm60$ $\mu$m versus $403\pm86$ $\mu$m, p<0.0001; Maximum BE thickness, $293\pm64$ $\mu$m versus $471\pm107$ $\mu$m, p<0.0001]. The scatter plot in Figure 3A shows the difference between the average BE thickness for the two groups. Figure 3B shows ROC curves using average

and maximum BE thickness to predict RFA treatment response. The area-under-the-curve (AUC) was 0.942 (p<0.001) and 0.934 (p<0.001) using the average and maximum BE thickness, respectively. An average BE thickness of 333 μm was determined from the ROC curve to achieve the best prediction accuracy. Using this decision threshold, a sensitivity of 92.3% (12/13), specificity of 85% (17/20), PPV of 80%, NPV of 94.4% and an accuracy of 87.9% (29/33) was obtained for predicting treatment response evaluated by the presence or absence of endoscopically visible residual BE at follow-up visit using the average BE thickness measured with OCT prior to the RFA treatment (Table 2). Considering only the patients with dysplastic BE (19/33), a sensitivity of 100% (9/9), specificity of 90% (9/10), PPV of 90%, NPV of 100% and an accuracy of 94.7% (18/19) was obtained for predicting treatment response evaluated by the presence or absence of endoscopically visible residual BE at the follow-up visit using the average BE thickness measured with OCT prior to RFA treatment. The BE thickness measured with OCT was not correlated with the length of the BE (p=0.88) or the number of prior RFA treatments (p=0.24).

A BE thickness of over 333 μm was also found to correlate with the presence of residual glands immediately after RFA [Table 3, sensitivity: 91.7% (11/12), specificity: 85% (17/20), PPV: 78.6%, NPV: 94.4%, and accuracy: 87.5% (28/32)]. Note that one subject was excluded from this analysis due to the lack of OCT images immediately after RFA. Finally, the presence of residual glands observed with OCT immediately after RFA was found to be another predictor of the RFA treatment response (Table 4). Sensitivity of 83.3% (10/12), specificity of 95% (19/20), PPV of 90.9%, NPV of 90.5% and an accuracy of 90.6% (29/32) was achieved when using the presence of residual glands visible on OCT immediately after RFA to predict the presence of endoscopically visible residual BE at follow-up.

## Discussion

While endoscopic 3D-OCT does not possess the same magnification or contrast as conventional histopathology, it can visualize tissue microstructure *in vivo* over a large field of view and provides real-time, depth-resolved information with micron scale resolution. Each 3D-OCT dataset in our study covers ~160 mm$^2$ in the distal esophagus. Although this is only a fraction of the field observed with white light endoscope it is many times larger than the field covered by pinch biopsy and 3D-OCT provides complementary information about BE thickness as well as tissue morphology. This is especially important immediately after the RFA treatment, when the endoscopic imaging field is covered with blood and tissue debris. Due to the limited visibility immediately after the RFA treatment, it is difficult to evaluate the presence of residual glands or unburned BE using white light endoscopy or NBI. Similarly, imaging modalities that require contrast agents such as confocal endomicroscopy have limited use since extravasation of the contrast obliterates the viewing area after RFA. However, as demonstrated, residual glandular structures can be observed using 3D-OCT.

In this study, 3D-OCT identified structural markers, including the thickness of the BE epithelium prior to RFA and the presence of residual glands immediately after RFA, which might be used to predict RFA treatment response at follow-up with high accuracy. We found that patients with an average BE thickness of over 333 μm were likely to have endoscopically visible residual BE at the follow-up visit 6-8 weeks after the RFA treatment. This result was not surprising, however, since the dosage of the RFA treatment has been set to achieve best efficacy with minimum injury depth.[6, 31] The energy delivery of a standard RFA application might not reach deep enough when the BE epithelium is thick. There are other possible confounding variables that may contribute to depth variation or incompleteness of the ablation, including variation of the RFA electrode contact with the esophagus and coagulated/sloughing debris building up on the electrode surface with

repeated ablations in a patient.[31] Indeed, we found a correlation between the BE epithelium thickness and the presence of residual glands immediately after RFA, suggesting not all RFA applications were effective. Insufficient energy delivery at the treatment sites or leaving BE unburned may be factors that lead to endoscopically visible residual BE at follow-up.

The efficacy of ablation therapies is generally assessed by follow-up endoscopy 6-8 weeks after RFA,[11-13] and patients undergo repeated ablation if residual BE is observed. Our results suggest that patient response rate may be stratified based on the BE thickness measured before RFA. Using this structural marker, it may be possible to adjust RFA treatment for each patient to optimize response. For patients with thicker BE epithelium, a more rigorous ablation may be required. This may involve a thorough cleaning of the ablation catheter and treatment areas to remove debris between the two sets of ablations, and if indicated, increased dosage for the RFA treatment. The ability of OCT to differentiate residual glands from normal tissue structures and debris caused by the ablation may also provide immediate information about the RFA treatment for the endoscopist. This may enable real-time evaluation of ablation depth and identification of regions requiring further treatment. The RFA treatment might be guided to further improve the efficacy of each ablation procedure. As a result, the number of treatment sessions might be reduced to reduce overall treatment time, patient anxiety and health care cost.

Fourteen non-dysplasia patients were enrolled in the current study. However, RFA treatment for patients with non-dysplastic BE is still debatable. According to the clinical guidelines for the management of Barrett's esophagus,[32, 33] endoscopic ablation therapies are only recommended for patients with high-grade dysplasia. Two recent large cohort studies from Northern Ireland and Denmark showed that the annual risk for adenocarcinoma in non-dysplastic BE was less than 0.2%, suggesting RFA treatment for patients with non-dysplastic BE holds no benefit.[34, 35] However, an earlier study performed in the U.S. Veteran population, and perhaps better reflective of this study population, showed a relatively higher annual risk for adenocarcinoma in non-dysplastic BE patients.[36] The National Cancer Institute estimates that the incidence of esophageal cancer in the general population of the United States (all races, both sexes, all ages) is approximately 4.5 per 100,000 (0.0045%).[37] Hence the incidence of esophageal cancer for patients with non-dysplastic BE still appears to be much higher than the general population.

Surveillance endoscopy with biopsy is recommended for patients with low-grade dysplasia or non-dysplastic BE. However, due to the recognized limitations of the surveillance strategy, such as biopsy sampling errors, lack of compliance with surveillance protocols, cost-utility considerations, and failure to avert cancer in many cases, endoscopic therapies intended to completely remove low-grade dysplasia and non-dysplastic BE can be considered as alternative strategies.[9] Indeed, recent studies have shown that complete eradication of intestinal metaplasia (CE-IM) can be achieved in 92% of patients with non-dysplastic BE at 5-year follow-up after RFA treatment.[9] In this study, the BE epithelial thickness was found to be a strong predictor for RFA treatment response in all patients with or without dysplastic BE, indicating that this structural marker can be useful regardless of the dysplasia status of the patients.

There are several limitations in the current study. First, the study was limited to a cohort of patients with short-segment BE. This was done because the OCT system had a limited pull back imaging length and it was desirable to image the GEJ in each data set in order to enable consistent placement of the OCT imaging catheter. Future OCT systems will be able to acquire larger data sizes and we plan to extend the study to patients with long segment BE and evaluate the efficacy of circumferential RFA treatment. The study was also focused on

patients receiving Halo90 ablation rather than Halo360, to be consistent with the actual ablation method. In addition, the dysplasia status of the patients was evaluated before the patients went through the initial RFA treatment. As presented in Table 1, on average 2.4 and 1.7 RFA procedures were performed before the time of OCT imaging for patients in the CE-IM and non-CE-IM groups, respectively. Biopsies were generally not performed at time of RFA and OCT imaging to confirm the dysplasia status. Variations in disease severity of the patients at the time of treatment may be a cofounding variable for treatment response. Future studies will be conducted to investigate the relation between the BE mucosal thickness and treatment response in patients with different dysplasia status.

Secondly, the thickness of BE epithelium may vary if the contact pressure of the OCT catheter on the tissue changes. An *ex vivo* study using human colon tissues reported that the epithelium thickness was reduced when the contact pressure is increased.[38] This effect may induce variability in the BE thickness measurement. In the current study, the OCT catheter was in contact with the esophagus with the endoscope at the neutral position and the esophagus was deflated during imaging acquisition. The esophagus naturally wrapped around the OCT catheter to maintain a consistent catheter contact for all patients. More detailed quantitative investigations are needed to understand the influence of catheter contact pressure on the BE thickness measurement.

Thirdly, while OCT structural markers may predict RFA treatment response, the current study does not address whether the RFA treatment efficacy can be improved and the number of treatments reduced using structural information provided by 3D-OCT. A rigorous longitudinal study is needed to further establish the utility of endoscopic 3D-OCT for guiding RFA treatment of BE in clinical practice.

Finally, although the imaging coverage of the current 3D-OCT catheter is significantly larger than standard biopsy, a single 3D-OCT scan only covered about one sixth of the circumference of the distal esophagus. If unburned BE or residual glands were missed by 3D-OCT immediately after RFA, the patient might fail to achieve CE-IM at follow-up even though OCT imaging may still predict complete response. To overcome these potential sampling errors, multiple 3D-OCT sets will need to be acquired to achieve comprehensive coverage over different quadrants of the distal esophagus. Other OCT probe designs, such as balloon probes, may also be employed to improve coverage and reduce potential sampling errors in the future.

## Conclusion

Endoscopic 3D-OCT can identify structural markers, including the thickness of the BE epithelium prior to RFA and the presence of residual glands immediately after RFA. These markers are promising predictors of RFA treatment response at follow up in patients with short-segment BE. 3D-OCT may provide valuable information which will enable endoscopists to make real-time treatment decisions improving the efficacy of RFA treatment and reducing the number of required treatments in the future.

## Supplementary Material

Refer to Web version on PubMed Central for supplementary material.

## Acknowledgments

## References

1. Odze RD, Lauwers GY. Histopathology of Barrett's esophagus after ablation and endoscopic mucosal resection therapy. Endoscopy. 2008; 40:1008–1015. [PubMed: 19065484]

2. Bergman JJGHM. Radiofrequency Ablation - Great for Some or Justified for Many? New England Journal of Medicine. 2009; 360:2353–2355. [PubMed: 19474433]

3. Ell C, Pech O, May A. Radiofrequency Ablation in Barrett's Esophagus. New England Journal of Medicine. 2009; 361:1021–1021. [PubMed: 19726777]

4. Shaheen NJ, Sharma P, Overholt BF, Wolfsen HC, Sampliner RE, Wang KK, Galanko JA, Bronner MP, Goldblum JR, Bennett AE, Jobe BA, Eisen GM, Fennerty MB, Hunter JG, Fleischer DE, Sharma VK, Hawes RH, Hoffman BJ, Rothstein RI, Gordon SR, Mashimo H, Chang KJ, Muthusamy VR, Edmundowicz SA, Spechler SJ, Siddiqui AA, Souza RF, Infantolino A, Falk GW, Kimmey MB, Madanick RD, Chak A, Lightdale CJ. Radiofrequency Ablation in Barrett's Esophagus with Dysplasia. New England Journal of Medicine. 2009; 360:2277–2288. [PubMed: 19474425]

5. Pouw R, Gondrie J, Sondermeijer C, ten Kate F, van Gulik T, Krishnadath K, Fockens P, Weusten B, Bergman J. Eradication of Barrett Esophagus with Early Neoplasia by Radiofrequency Ablation, with or without Endoscopic Resection. Journal of Gastrointestinal Surgery. 2008; 12:1627–1637. [PubMed: 18704598]

6. Dunkin B, Martinez J, Bejarano P, Smith C, Chang K, Livingstone A, Melvin W. Thin-layer ablation of human esophageal epithelium using a bipolar radiofrequency balloon device. Surgical Endoscopy. 2006; 20:125–130. [PubMed: 16333533]

7. Sharma VK, Wang KK, Overholt BF, Lightdale CJ, Fennerty MB, Dean PJ, Pleskow DK, Chuttani R, Reymunde A, Santiago N, Chang KJ, Kimmey MB, Fleischer DE. Balloon-based, circumferential, endoscopic radiofrequency ablation of Barrett's esophagus: 1-year follow-up of 100 patients (with video). Gastrointestinal Endoscopy. 2007; 65:185–195. [PubMed: 17258973]

8. Shaheen NJ, Overholt BF, Sampliner RE, Wolfsen HC, Wang KK, Fleischer DE, Sharma VK, Eisen GM, Fennerty MB, Hunter JG, Bronner MP, Goldblum JR, Bennett AE, Mashimo H, Rothstein RI, Gordon SR, Edmundowicz SA, Madanick RD, Peery AF, Muthusamy VR, Chang KJ, Kimmey MB, Spechler SJ, Siddiqui AA, Souza RF, Infantolino A, Dumot JA, Falk GW, Galanko JA, Jobe BA, Hawes RH, Hoffman BJ, Sharma P, Chak A, Lightdale CJ. Durability of Radiofrequency Ablation in Barrett's Esophagus With Dysplasia. Gastroenterology. 2011; 141:460–468. [PubMed: 21679712]

9. Fleischer DE, Overholt BF, Sharma VK, Reymunde A, Kimmey MB, Chuttani R, Chang KJ, Muthasamy R, Lightdale CJ, Santiago N, Pleskow DK, Dean PJ, Wang KK. Endoscopic radiofrequency ablation for Barrett's esophagus: 5-year outcomes from a prospective multicenter trial. Endoscopy. 2010; 42:781–789. [PubMed: 20857372]

10. Vaccaro B, Gonzalez S, Poneros J, Stevens P, Capiak K, Lightdale C, Abrams J. Detection of Intestinal Metaplasia After Successful Eradication of Barrett's Esophagus with Radiofrequency Ablation. Digestive Diseases and Sciences. 2011; 56:1996–2000. [PubMed: 21468652]

11. Barr H, Krasner N, Boulos PB, Chatlani P, Bown SG. PHOTODYNAMIC THERAPY FOR COLORECTAL-CANCER - A QUANTITATIVE PILOT-STUDY. British Journal of Surgery. 1990; 77:93–96. [PubMed: 2302524]

12. Johnston MH. Cryotherapy and other newer techniques. Gastrointest Endosc Clin N Am. 2003; 13:491–504. [PubMed: 14629105]

13. Barr H, Stone N, Rembacken B. Endoscopic therapy for Barrett's oesophagus. Gut. 2005; 54:875–884. [PubMed: 15888799]

14. Das A, Wells C, Kim HJ, Fleischer DE, Crowell MD, Sharma VK. An economic analysis of endoscopic ablative therapy for management of nondysplastic Barrett's esophagus. Endoscopy. 2009; 41:400–408. [PubMed: 19418393]

15. Inadomi JM, Somsouk M, Madanick RD, Thomas JP, Shaheen NJ. A Cost-Utility Analysis of Ablative Therapy for Barrett's Esophagus. Gastroenterology. 2009; 136:2101–2114.e6. [PubMed: 19272389]

16. Huang D, Swanson EA, Lin CP, Schuman JS, Stinson WG, Chang W, Hee MR, Flotte T, Gregory K, Puliafito CA, Fujimoto JG. Optical Coherence Tomography. Science. 1991; 254:1178–1181. [PubMed: 1957169]

17. Tearney GJ, Brezinski ME, Southern JF, Bouma BE, Boppart SA, Fujimoto JG. Optical biopsy in human gastrointestinal tissue using optical coherence tomography. The American journal of gastroenterology. 1997; 92:1800–4. [PubMed: 9382040]

18. Bouma BE, Tearney GJ, Compton CC, Nishioka NS. High-resolution imaging of the human esophagus and stomach in vivo using optical coherence tomography. Gastrointestinal endoscopy. 2000; 51((4) Pt 1):467–74. [PubMed: 10744824]

19. Li XD, Boppart SA, Van Dam J, Mashimo H, Mutinga M, Drexler W, Klein M, Pitris C, Krinsky ML, Brezinski ME, Fujimoto JG. Optical coherence tomography: advanced technology for the endoscopic imaging of Barrett's esophagus. Endoscopy. 2000; 32:921–30. [PubMed: 11147939]

20. Poneros JM. Diagnosis of Barrett's esophagus using optical coherence tomography. Gastrointest Endosc Clin N Am. 2004; 14:573–88. x. [PubMed: 15261203]

21. Evans JA, Nishioka NS. The use of optical coherence tomography in screening and surveillance of Barrett's esophagus. Clin Gastroenterol Hepatol. 2005; 3:S8–11. [PubMed: 16013005]

22. Chen Y, Aguirre AD, Hsiung PL, Desai S, Herz PR, Pedrosa M, Huang Q, Figueiredo M, Huang SW, Koski A, Schmitt JM, Fujimoto JG, Mashimo H. Ultrahigh resolution optical coherence tomography of Barrett's esophagus: preliminary descriptive clinical study correlating images with histology. Endoscopy. 2007; 39:599–605. [PubMed: 17611914]

23. Adler DC, Zhou C, Tsai TH, Lee HC, Becker L, Schmitt JM, Huang Q, Fujimoto JG, Mashimo H. Three-dimensional optical coherence tomography of Barrett's esophagus and buried glands beneath neosquamous epithelium following radiofrequency ablation. Endoscopy. 2009; 41:773–776. [PubMed: 19746317]

24. Suter MJ, Vakoc BJ, Yachimski PS, Shishkov M, Lauwers GY, Mino-Kenudson M, Bouma BE, Nishioka NS, Tearney GJ. Comprehensive microscopy of the esophagus in human patients with optical frequency domain imaging. Gastrointestinal Endoscopy. 2008; 68:745–753. [PubMed: 18926183]

25. Adler DC, Zhou C, Tsai TH, Schmitt J, Huang Q, Mashimo H, Fujimoto JG. Three-dimensional endomicroscopy of the human colon using optical coherence tomography. Optics Express. 2009; 17:784–796. [PubMed: 19158891]

26. Zhou C, Adler DC, Becker L, Chen Y, Tsai TH, Figueiredo M, Schmitt JM, Fujimoto JG, Mashimo H. Effective treatment of chronic radiation proctitis using radiofrequency ablation. Therapeutic Advances in Gastroenterology. 2009; 2:149–156. [PubMed: 20593010]

27. Isenberg G, Sivak MV, Chak A, Wong RCK, Willis JE, Wolf B, Rowland DY, Das A, Rollins A. Accuracy of endoscopic optical coherence tomography in the detection of dysplasia in Barrett's esophagus: a prospective, double-blinded study. Gastrointestinal Endoscopy. 2005; 62:825–831. [PubMed: 16301020]

28. Zhou C, Tsai TH, Lee HC, Kirtane T, Figueiredo M, Tao YK, Ahsen OO, Adler DC, Schmitt JM, Huang Q, Fujimoto JG, Mashimo H. Characterization of Buried Glands Pre- and Post-Radiofrequency Ablation using Threedimensional Optical Coherence Tomography. Gastrointestinal endoscopy. in press.

29. Sharma P, Dent J, Armstrong D, Bergman JJGHM, Gossner L, Hoshihara Y, Jankowski JA, Junghard O, Lundell L, Tytgat GNJ, Vieth M. The Development and Validation of an Endoscopic Grading System for Barrett's Esophagus: The Prague C & M Criteria. Gastroenterology. 2006; 131:1392–1399. [PubMed: 17101315]

30. Adler DC, Chen Y, Huber R, Schmitt J, Connolly J, Fujimoto JG. Three-dimensional endomicroscopy using optical coherence tomography. Nature Photonics. 2007; 1:709–716.

31. Trunzo J, McGee M, Poulose B, Willis J, Ermlich B, Laughinghouse M, Champagne B, Delaney C, Marks J. A feasibility and dosimetric evaluation of endoscopic radiofrequency ablation for

human colonic and rectal epithelium in a treat and resect trial. Surgical Endoscopy. 2011; 25:491–496. [PubMed: 20652324]

32. Wang KK, Sampliner RE. Updated Guidelines 2008 for the Diagnosis, Surveillance and Therapy of Barrett's Esophagus. Am J Gastroenterol. 2008; 103:788–797. [PubMed: 18341497]

33. Spechler SJ, Sharma P, Souza RF, Inadomi JM, Shaheen NJ. American Gastroenterological Association Technical Review on the Management of Barrett's Esophagus. Gastroenterology. 2011; 140:e18–e52. [PubMed: 21376939]

34. Bhat S, Coleman HG, Yousef F, Johnston BT, McManus DT, Gavin AT, Murray LJ. Risk of Malignant Progression in Barrett's Esophagus Patients: Results from a Large Population-Based Study. Journal of the National Cancer Institute. 2011

35. Hvid-Jensen F, Pedersen L, Drewes ArM, Sørensen HT, Funch-Jensen P. Incidence of Adenocarcinoma among Patients with Barrett's Esophagus. New England Journal of Medicine. 2011; 365:1375–1383. [PubMed: 21995385]

36. Spechler SJ, Lee E, Ahnen D, Goyal RK, Hirano I, Ramirez F, Raufman JP, Sampliner R, Schnell T, Sontag S, Vlahcevic ZR, Young R, Williford W. Long-term outcome of medical and surgical therapies for gastroesophageal reflux disease - Follow-up of a randomized controlled trial. Jama-Journal of the American Medical Association. 2001; 285:2331–2338.

37. Howlader, N.; Noone, AM.; Krapcho, M.; Neyman, N.; Aminou, R.; Waldron, W.; Altekruse, SF.; Kosary, CL.; Ruhl, J.; Tatalovich, Z.; Cho, H.; Mariotto, A.; Eisner, MP.; Lewis, DR.; Chen, HS.; Feuer, EJ.; Cronin, KA.; Edwards, BK., editors. SEER Cancer Statistics Review, 1975-2008. National Cancer Institute; Bethesda, MD: 2011. http://seer.cancer.gov/csr/1975_2008/, based on November 2010 SEER data submission, posted to the SEER web site

38. Westphal V, Rollins AM, Willis J, Sivak MV, Izatt JA. Correlation of endoscopic optical coherence tomography with histology in the lower-GI tract. Gastrointest Endosc. 2005; 61:537–46. [PubMed: 15812406]

## Acronyms

| | |
|---|---|
| **3D** | three dimensional |
| **AUC** | area under the curve |
| **BE** | Barrett's esophagus |
| **CE** | complete eradication |
| **CE-D** | complete eradication of dysplasia |
| **CE-IM** | complete eradication of intestinal metaplasia |
| **EGD** | esophagogastroduodenoscopy |
| **GEJ** | gastroesophageal junction |
| **GI** | gastrointestinal |
| **HGD** | high grade dysplasia |
| **IM** | intestinal metaplasia |
| **LGD** | low grade dysplasia |
| **LP** | lamina propria |
| **MM** | muscularis mucosa |
| **NBI** | narrow band imaging |
| **NDBE** | non-dysplastic Barrett's esophagus |
| **NPV** | negative predicting value |
| **OCT** | optical coherence tomography |

| **PPI** | proton pump inhibitor |
| **PPV** | positive predicting value |
| **RFA** | radiofrequency ablation |
| **ROC** | receiver operator characteristic |
| **SD** | standard deviation |
| **VABHS** | Veterans Affairs Boston Healthcare System |

**Take-home Message**

Thicker BE epithelium measured by 3D-OCT prior to ablation is associated with reduced treatment response of RFA assess at follow up. The presence of residual glands immediately after RFA is also correlated with thicker BE prior to RFA as well as with treatment response at follow up. 3D-OCT provides a useful tool for for identifying factors are associated with RFA treatment response and may improve the effectiveness of therapy to reduce the number of treatments required to achieve complete response in the future.
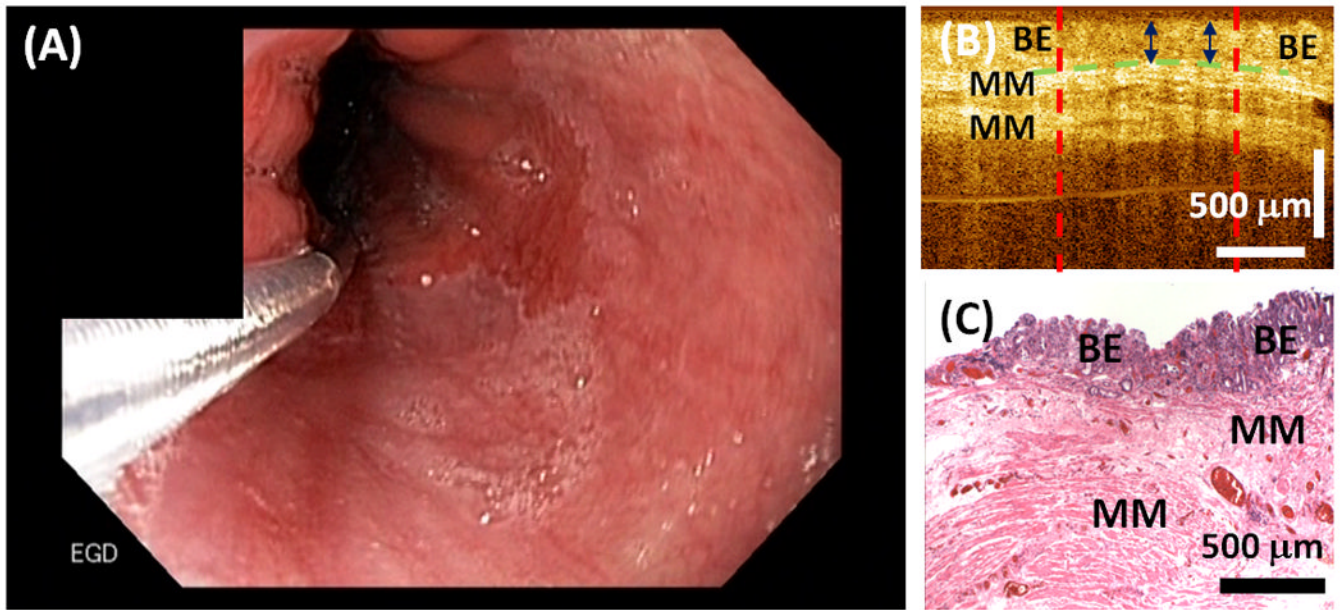
**Figure 1.**
(A) Representative endoscopic image of the GEJ before RFA treatment. (B) Representative cross-sectional OCT image and (C) corresponding histology illustrating the BE epithelium thickness measurement.
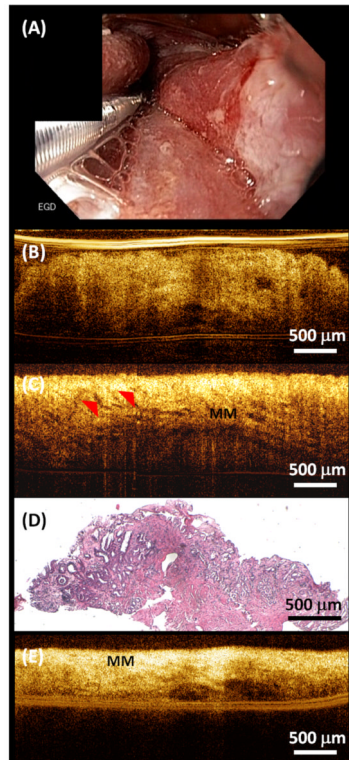
**Figure 2.**
(A) Representative endoscopic image of the GEJ immediately after RFA treatment. (B) Representative cross-sectional OCT image showing unburned BE epithelium missed by RFA. (C) Representative cross-sectional OCT image showing residual glands after RFA. (D) Corresponding histology of (C) confirming residual BE glands after RFA. (E) Representative cross-sectional OCT image showing effective RFA treatment. The entire BE epithelium was ablated, resulting in exposed muscularis mucosa (MM) on the surface.
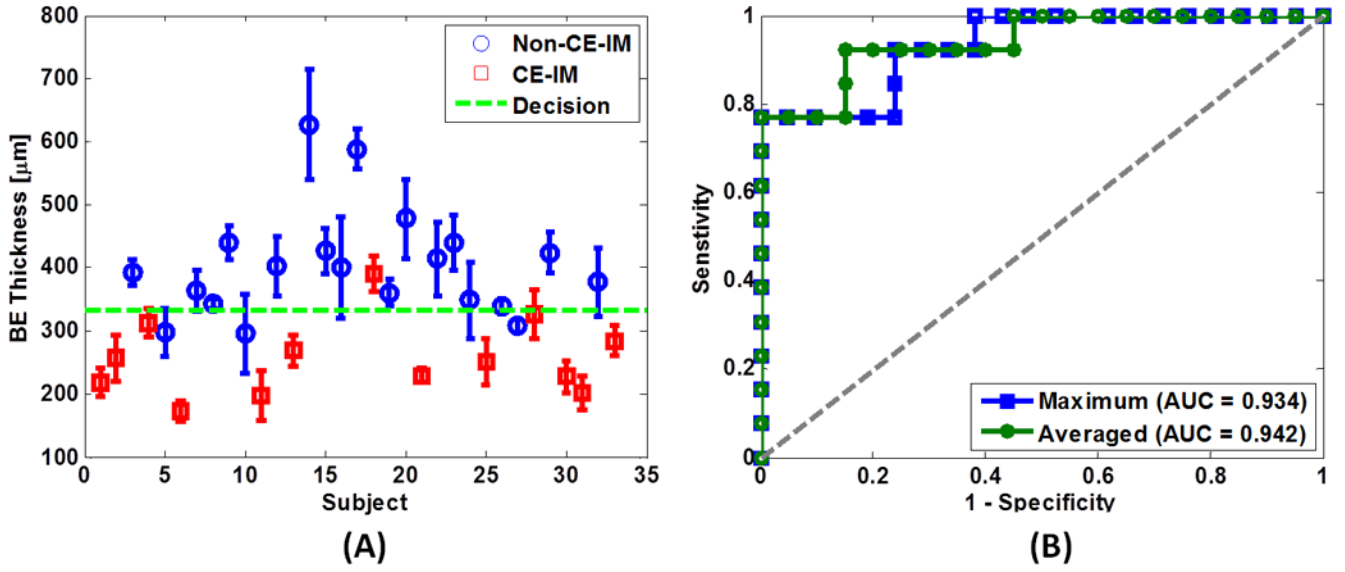
**Figure 3.**
(A) Scatter plot of the average BE epithelium thickness measured by OCT. Blue circles: Non-CE-IM group; Red crosses: CE-IM group; Green dotted line: discrimination threshold at 333 μm as determined from the average BE thickness ROC curve in (B). (B) ROC curves of treatment response prediction using average (green) and maximum (blue) BE thickness. The area-under-the-curve (AUC) values were 0.942 (p<0.001) and 0.934 (p<0.001) using the average and maximum BE thickness, respectively.

**Table 1**

**Subject demographic information**

|  | CE-IM Group | Non-CE-IM Group | P Value |
|---|---|---|---|
| Enrollment | 13 | 20 |  |
| Gender, male/female | 12/1 | 20/0 |  |
| Race | 13 Caucasian | 20 Caucasian |  |
| Age [years] |  |  |  |
| Mean (SD) | 64.9 (7.7) | 65.6 (15.8) | 0.86 |
| Range | 51-77 | 33-92 |  |
| Initial Diagnosis |  |  |  |
| BE w/o dysplasia | 4 | 10 |  |
| LGD | 2 | 4 |  |
| HGD | 7 | 6 |  |
| Prior RFA Treatments |  |  |  |
| Mean (SD) | 2.4 (1.9) | 1.7 (1.6) | 0.34 |
| Range | 0-7 | 0-6 |  |
| Length of BE [cm] |  |  |  |
| Mean (SD) | 1.3 (0.8) | 1.0 (0.7) | 0.29 |
| Range | 0.5-3 | 0.5-3 |  |

**Table 2**

**Average BE thickness measured by OCT before RFA predicts the presence or absence of endoscopically visible residual BE at follow-up visit**

| | Absence of Residual BE at Follow-up | Presence of Residual BE at Follow-up | Total | |
|---|---|---|---|---|
| Average BE Thickness < 333 μm | 12 | 3 | 15 | PPV = 80% |
| Average BE Thickness 333 μm | 1 | 17 | 18 | NPV = 94.4% |
| Total | 13 | 20 | 33 | |
| | Sensitivity = 92.3% | Specificity = 85% | Accuracy = 87.9% | |

**Table 3**

**Average BE thickness measured by OCT before RFA predicts the presence or absence of residual glands measured by OCT immediately after RFA**

| | Absence of Residual Glands Immediately after RFA | Presence of Residual Glands Immediately after RFA | Total | |
|---|---|---|---|---|
| Average BE Thickness < 333 μm | 11 | 3 | 14 | PPV = 78.6% |
| Average BE Thickness 333 μm | 1 | 17 | 18 | NPV = 94.4% |
| Total | 12 | 20 | 32 | |
| | Sensitivity = 91.7% | Specificity = 85% | Accuracy = 87.5% | |

**Table 4**

**Presence or absence of residual glands measured by OCT immediately after RFA predicts the presence or absence of endoscopically visible residual BE at follow-up visit**

|  | Absence of Residual BE at Follow-up | Presence of Residual BE at Follow-up | Total |  |
|---|---|---|---|---|
| Absence of Residual Glands Immediately after RFA | 10 | 1 | 11 | PPV = 90.9% |
| Presence of Residual Glands Immediately after RFA | 2 | 19 | 21 | NPV = 90.5% |
| Total | 12 | 20 | 32 |  |
|  | Sensitivity = 83.3% | Specificity = 95% | Accuracy = 90.6% |  |